JGI Journal of Global Innovation

BIOprospectum Open access publishing

Article

Artificial neural networks applied in the optimization of the adsorption of thin films of phthalocyanines

Aline Márcia de Oliveira Farias [1,5], Emanuel Airton de Oliveira Farias [1], Carla Eiras [2], Durcilene Alves da Silva [1], Ricardo A. L. Rabêlo [3] and Dario Brito Calçada [4,5]*

1. Núcleo de Pesquisa em Biodiversidade e Biotecnologia, BIOTEC, Campus Ministro Reis Velloso, UFPI, Parnaíba, PI, Brasil.
2. Laboratório Interdisciplinar de Materiais Avançados - LIMAV, Campus Ministro Petrônio Portela, CT, UFPI, Teresina-PI, Brasil.
3. Universidade Federal do Piauí (UFPI), Centro de Ciências da Natureza (CCN), Departamento de Computação (DC), Teresina-PI, Brasil.
4. Universidade de São Paulo (USP), Instituto de Computação e Matemática Computacional (ICMC), Laboratório de Inteligência Computacional (LABIC), São Carlos-SP, Brasil
5. Universidade Estadual do Piauí (UESPI), Campus Alexandre Alves de Oliveira, Parnaíba-PI, 64200-000, Brasil
*Correspondence: dariobcalcada@gmail.com; Tel.: +55-86-99946-9867

Received: 02 Jan 2019; Accepted: 15 May 2020; Published: 28 June 2020.

Abstract: This paper presents the study of Artificial Neural Networks (ANNs) as learning, simulation and optimization systems for the production of thin films. In this sense, thin films based on Fe (II) tetrasulfonated phthalocyanine (FeTSPc) were prepared by layer-by-layer (LbL) self-assembling technique and characterized by UV-Vis spectroscopy. The results obtained by the training of ANNs demonstrate a good correlation between the absorbance and the parameters involved during the production process of the films, such as FeTsPC concentration, solution pH and adsorption time for these films.

Keywords: Artificial Neural Networks; Multi-Layer Perceptron; Fine Films; Layer by Layer; Phthalocyanine

1. Introduction

The chemistry of materials studies about the synthesis, characterization, and investigation of the properties of several compounds, as well as the functionalization of the same. Since the properties of the materials are strongly affected by the size of the particles that compose them, a new follow-up of this area gained considerable importance from the XX century: the research in nanomaterials. In this sense, the scope of nanoscience or nanotechnology is to investigate the properties of materials at the nanoscale for the development of new technologies and improvement of existing ones [1-3].

Among the range of compounds used in the construction of nanomaterials, we highlight the phthalocyanines, which can be complexed as intense staining and high chemical and thermal stability, as well as semiconductor properties. Due to these properties, these compounds are currently used as pigments, photosensitizers, sensors and in electronic components and photonic devices, such as solar cells, optical memory, as well as being used in areas such as catalysis and photodynamic cancer therapy [4-6].

Most of the phthalocyanine-based devices are developed from their immobilization in the form of thin films [7]. By thin films, the condensed matter is arranged in layers that are immobilized on a solid surface, known as a substrate, whose layers are in the range of fractions of a nanometer to several micrometers thick [8]. Several techniques have been employed in the production of these films, such as Chemical Deposition and Steam Physics [9], Sol-gel [9], Langmuir-Blodgett (LB), Casting, spin coating [10] in addition to the layer-by-layer (LbL) self-assembling method [12].

The LbL technique stands out because it is a highly versatile technique, allowing the production of ultrafine films of different types of materials, in a simple and economically feasible way, besides providing the structures with a high degree of an organization at a molecular level [12]. This technique consists of the alternating adsorption of layers of materials of opposite charges, which are held together by electrostatic

attraction [13-14]. One of the materials that have been of interest for the construction of films is tetrasulfonated Fe (II) Phthalocyanine (FeTSPc), a polyanionic material (contains negative charges) [15-16].

The adsorption of FeTSPc and the vast majority of the materials is influenced by several thermodynamic factors, among them the contact time with the substrate, the concentration of the precursor solution and its pH [17]. The interest in studying the adsorptive properties of materials in the form of films is the objective of improving the preparation conditions of these films, thus enabling better control of their final properties [18-19].

Ultraviolet-Visible (UV-Vis) spectroscopy is one of the analytical methods most commonly used in analytical determinations in several areas. Using the UV-Vis technique, it is possible, for example, to follow the formation of a self-assembled film and to speculate on the amount of adsorbed material. Since according to the Beer-Lambert Law it is possible to relate the absorbance that occurs in the wavelength characteristic of the molecule present in the film, with the thickness of the absorber medium (in this case, the film) and the concentration of adsorbed material [20-23].

The need to obtain FeTSPc thin films with desirable characteristics is evident, based on the preparation parameters of such films, to obtain a higher degree of reproducibility. Due to the difficulty of correlation between the different experimental parameters with the final characteristics of thin films, a large set of data and experiments becomes necessary for the optimization of the production process of these films [21]; [24-25].

An alternative to simulate and improve the preparation parameters of FeTSPc films is the use of computational techniques, such as Artificial Neural Networks (ANNs). ANNs also called connectionist networks, distributed parallel processing and neural computing, are computational models inspired by the nervous system of living beings. The ANNs are inserted within the area known as Computational Intelligence (CI) and seek, through techniques inspired by nature, the development of artificial intelligent systems that imitate some aspects of human behavior, such as perception, reasoning, learning, evolution, and adaptation [26-27].

ANNs are employed in a variety of engineering and science problem-solving applications. Among these applications, it is worth mentioning that of a universal approximation of functions, whose purpose of the network is to map the functional relationship between the variables of a system from a known set of its representative values. This technique allows its application in the mapping of processes whose modeling by conventional techniques are difficult to obtain [28-31].

The objective of this work was to use ANNs to aid in the adsorption process of films based on FeTSPc using data collected experimentally.

2. Materials and Methods

2.1 Hydrophilization of substrates for film deposition

For the spectroscopic studies, we used standard glass slides (BK7). Before adsorption of the FeTSPc films, we subjected these substrates to a cleaning step called hydrophilization, which consists in the removal of grease and dirt from the surface of these substrates. The cleaning process consisted of the following steps:

It was mixed in a beaker: 5 ml ultrapure water (Mili-Q), 2 g KOH (potassium hydroxide) and 95 ml ethanol. The slides were placed in a Teflon slide basket, and then the basket was dipped into the prepared solution. Then, we left the solution under ultrasonic bath for 10 min. At the end of this time, the slides were washed with ultrapure water, placed in another beaker containing 100 ml of ultrapure water and left again on the ultrasound for 5 minutes. After this time, they were dried with the N2 flow (nitrogen gas) and then stored separately until the moment of its use.

2.2. Preparation of the solutions used for adsorption of FeTSPc

Several solutions prepared at concentrations of 0.5, 0.7 and 1.0 $g.L^{-1}$ adsorbed the FeTSPc. From each of these concentrations, we produced solutions with pHs of 2.8, 5.6, 8.2 and 10.5. The pH was adjusted by adding micro volumes of NaOH (0.1 $mol.L^{-1}$) or HCl ((0.1 $mol.L^{-1}$).

Hydrochlorinated polyallylamine (PAH) is a synthetic cationic polymer widely used in the preparation of LbL films. In this sense, PAH was used to treat the substrate with a positive polymer layer, thus allowing a higher number of active sites for FeTSPc adsorption via electrostatic interaction. The PAH solution was prepared at the concentration of 1.0 $g.L^{-1}$ in HCl pH 2.8 and stored in a dark glass bottle at room temperature (25 ° C).

A solution of HCl pH 2.8 was used as the wash solution in all experiments.

2.3. Preparation of FeTSPc layer-by-layer films

FeTSPc films were adsorbed onto standard glass slides using the LbL technique to evaluate which parameters favor higher adsorption of FeTSPc. In the diagram of Figure I, we can observe the scheme of preparation of the films.

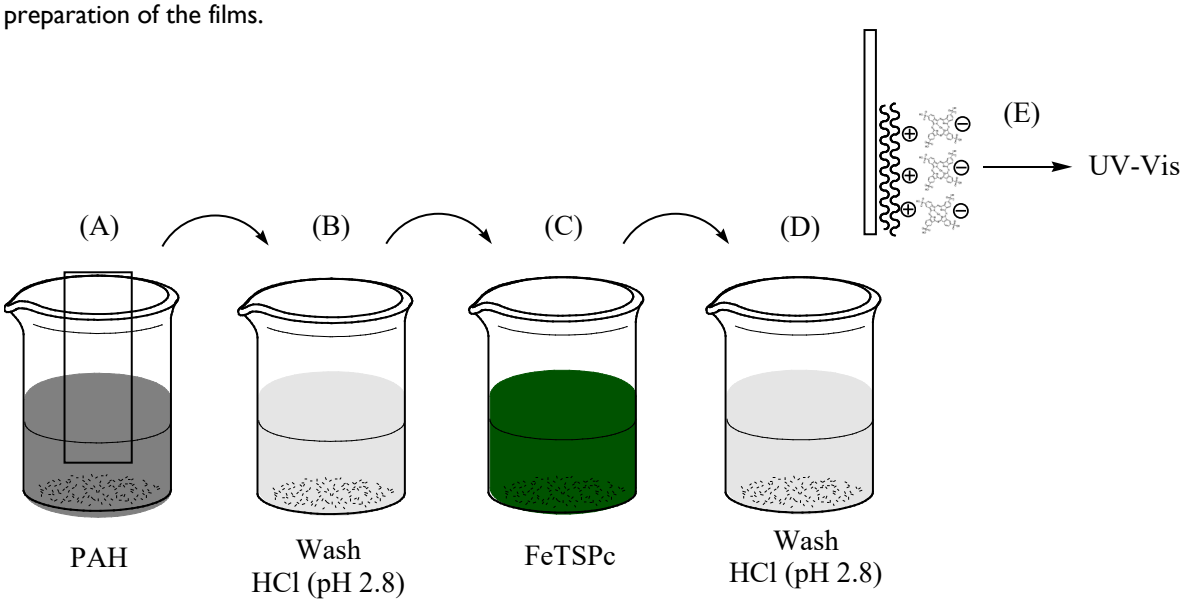

Figure 1. FeTSPc film preparation process. A) PAH (poly (allylamine hydrochlorinated)), B) HCl (hydrochloric acid), C) FeTSPc (Tetrasulfonated Fe (II) phthalocyanine), D) HCl (hydrochloric acid), E) UV-Vis (maximum absorbance obtained).

For the preparation of the films, we immersed a glass substrate previously in a solution of PAH for the treatment of the substrate (Figure I (a)). This step had the objective of treating the substrate, leaving it charged positively for better adsorption of FeTSPc. The concentration and pH of the PAH solution, respectively 0.1 $g.L^{-1}$ and 2.8, were kept fixed throughout the experiments. It is worth noting that PAH does not absorb in the UV-Vis region [32], and there is no risk of interference in the study of interest. In step (b) the substrate / PAH assembly was immersed in a wash solution to remove excess material that was not adsorbed in the adsorption step. Subsequently, the substrate treated with PAH was immersed in the FeTSPc solution (Figure I (c)), which was prepared under the pHs: 2.8, 5.6, 8.2, 10.5 and concentrations of 0.5, 0.7 and 1 $g.L^{-1}$ under different times of contact with the solution: 10, 20, 30, 60 and 90 min. A washing step was also performed for removal of the non-adsorbed FeTSPc (Figure I (d)). Finally, a substrate / PAH / FeTSPc film reading was performed on spectrometry in the UV-Vis region and the maximum absorbance value obtained was recorded (Figure I (e)). All washing steps were performed by drying with nitrogen (N2).

2.4. Characterization of FeTSPc Layer-by-Layer Films

The films produced were characterized by spectroscopy in the UV-Vis region, using a SHIMADZU UV-1800 spectrophotometer.

2.5. Implementation of artificial neural network

To create, train, validate and simulate ANNs, we used the MATLAB® software in version R2013a (8.1.0.604).

A Multi Layer Perceptron (MLP) artificial neural network was implemented in which the parameters involved in FeTSPc films production were used as input data: (a) FeTSPc concentration (0.5, 0.7 and 1.0 $g.L^{-1}$) ; (b) solution pH (2.8, 5.6, 8.2 and 10.5) and (c) time of contact with the solution (10, 20, 30, 60 and 90 min).

To evaluate the generalization of the network training, we divided the data set into a randomly selected training, validation and test set. Table I shows the number of data used in each of the analyzes.

Network training consists of adjusting the weights of the various layers so that the output matches the desired value for a given input. This process is repeated for all input vectors of the network until the mean square error of the network outputs is within an allowable value. Cross-validation is used to ensure network

generalization, ensuring that it can accurately respond to other inputs that were not used during training. The tests were performed with data that were not used in training or ANN validation. These data are used as a way of verifying the correct functioning of the network, as well as demonstrating its capacity for learning and generalization.

Table 1. The number of data used for training, validation and testing of ANNs.

	Amount of Experiments	%
Training	36	60
Validation	12	20
Testing	12	20
Total	60	100

The maximum and the minimum number of neurons present in the hidden layers and quantities of tests with each configuration was defined according to the Kolmogorov theorem [33]. Which states that a network of P inputs can be represented by P * 2 + 1 neurons in the hidden layer, in this way, the network architecture was defined as follows: three input variables, two intermediate layers and one output layer. In the first intermediate layer, the number of neurons varied from 2 to 7 and in the second, from 0 to 3 neurons (P * 2 + 1) / 2. We defined the total number of training times equal to 200, as well as the number of tests equal to 10 and cross-validations equal to 15.

It is noteworthy that a data normalization process was carried out, in which all input parameters were standardized in the range of 0.1 to 0.9.

An algorithm (Figure 2) was implemented to test different network configurations, analyzing the reproducibility and influence of the parameters in the final simulation results. The operation of the algorithm can be seen in Figure 2.

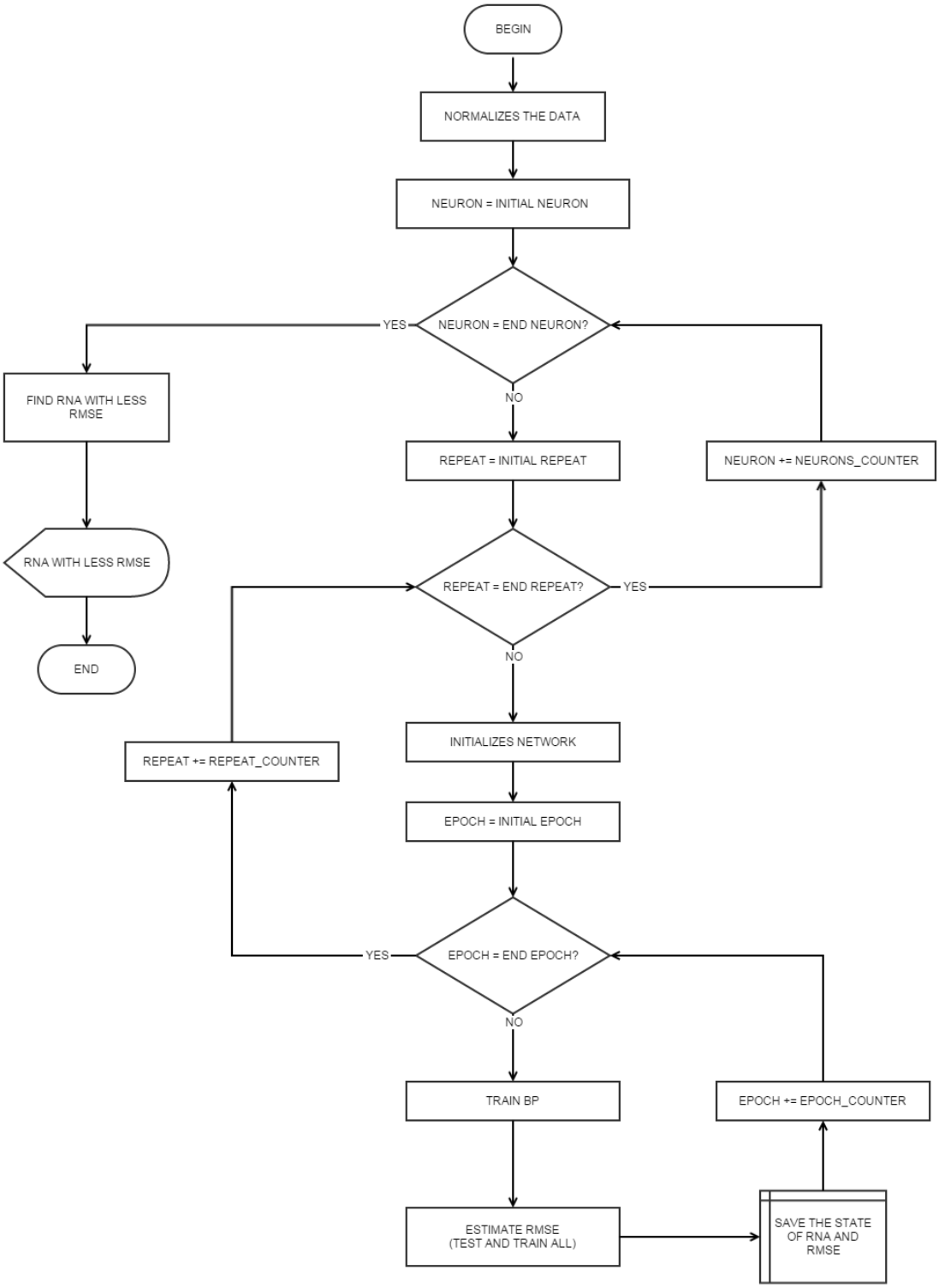

Figure 2. The algorithm used to train and analyze the error (Neuron = number of neurons in the intermediate layer, Epoch = number of epochs, Repeat = number of repetitions (initialization), BP = Backpropagation, RMSE = Square root of the mean square error (Mean Square Error)).

The algorithm consists of initializing a neural network with some X neurons, training it Y times, calculating the error and saving the state of the network at every instant. After training the maximum number of times, a new neural network is initialized with another number of neurons in the hidden layer. Repeat the procedure Z times (default value by the user). Thus, it is repeated Z times, neural networks that contain X neurons in the hidden layer, by Y times. All networks were stored (in all the states).

Finally, the algorithm finds the network that presented the smallest error and indicates to the user who it is. This algorithm generates different initial networks with the same number of neurons, to train them for Y times saving each value and at the end presents which one approached more of the training set and the test set.

3. Results and Discussion

3.1. Spectroscopic characterization in the ultraviolet-visible region (UV-Vis)

The process of formation of the self-produced films produced in this work was monitored by spectroscopy in the ultraviolet-visible region (UV-Vis). Phthalocyanines may present in the electron spectrum a band in the region of 350 nm and two or more bands in the region of 600 to 750 nm [34].

The self-styled FeTSPc films studied in this work presented bands in the region of 600 to 750 nm. These absorption bands are attributed to their 18 π electrons in the macrocyclic ring [35].

In this work, we try to establish the relationship between the concentration, the pH of the FeTSPc solution and the contact time of the substrate with the solution used during the FeTSPc thin films production process, with the absorbance value obtained. The absorbance is a parameter that is closely correlated with the amount of adsorbed material and the film thickness - Lambert-Beer Act (Equation1). Therefore, a higher absorbance is an indication that there is a more significant amount of FeTSPc adsorbed on the film.

$$Log\ (I_0/ I) = A = \varepsilon\, c\, l \qquad (1)$$

Where
A = absorbance;
ε = molecular absorption or extinction coefficient;
c = concentration of the absorbing material;
l = the thickness of the sample through which the light propagates.

In Table 2 all the parameters involved during the production of the thin films are listed, as well as the value of the final absorbance obtained.

Table 2. Parameters varied during the production of FeTSPc films.

Experiment	Concentration ($g.L^{-1}$)	pH	Contact time (min.)	Absorbance (u.a)
1	0.5	2.8	10	0.048
2	0.5	2.8	20	0.054
3	0.5	2.8	30	0.052
4	0.5	2.8	60	0.055
5	0.5	2.8	90	0.059
6	0.5	5.6	10	0.055
7	0.5	5.6	20	0.061
8	0.5	5.6	30	0.059
9	0.5	5.6	60	0.054
10	0.5	5.6	90	0.047
11	0.5	8.2	10	0.050
12	0.5	8.2	20	0.056
13	0.5	8.2	30	0.051
14	0.5	8.2	60	0.055
15	0.5	8.2	90	0.049
16	0.5	10.5	10	0.047
17	0.5	10.5	20	0.054
18	0.5	10.5	30	0.056
19	0.5	10.5	60	0.059
20	0.5	10.5	90	0.056

21	0.7	2.8	10	0.058
22	0.7	2.8	20	0.057
23	0.7	2.8	30	0.058
24	0.7	2.8	60	0.054
25	0.7	2.8	90	0.060
26	0.7	5.6	10	0.048
27	0.7	5.6	20	0.049
28	0.7	5.6	30	0.050
29	0.7	5.6	60	0.048
30	0.7	5.6	90	0.054
31	0.7	8.2	10	0.052
32	0.7	8.2	20	0.055
33	0.7	8.2	30	0.050
34	0.7	8.2	60	0.051
35	0.7	8.2	90	0.050
36	0.7	10.5	10	0.053
37	0.7	10.5	20	0.050
38	0.7	10.5	30	0.057
39	0.7	10.5	60	0.059
40	0.7	10.5	90	0.057
41	1	2.8	10	0.058
42	1	2.8	20	0.060
43	1	2.8	30	0.059
44	1	2.8	60	0.059
45	1	2.8	90	0.058
46	1	5.6	10	0.052
47	1	5.6	20	0.053
48	1	5.6	30	0.061
49	1	5.6	60	0.061
50	1	5.6	90	0.056
51	1	8.2	10	0.055
52	1	8.2	20	0.056
53	1	8.2	30	0.057
54	1	8.2	60	0.057
55	1	8.2	90	0.057
56	1	10.5	10	0.062
57	1	10.5	20	0.060
58	1	10.5	30	0.058
59	1	10.5	60	0.052
60	1	10.5	90	0.058

Based on Figure 3, it appears that the higher the concentration of the solution, the greater the absorbance value obtained. However, this observation is only seen for this configuration, that is, with pH 10.5 and time of contact of the substrate with the solution of 10 minutes, once changing one of the parameters: pH or time, an idea was verified contrary, as can be seen in Table 2.

The concentration variation does not cause a similar variation in the absorbance, so the concentration behavior about the absorbance is not mathematically detectable without some correlated technique, for example, the one used in this work: Artificial Neural Networks

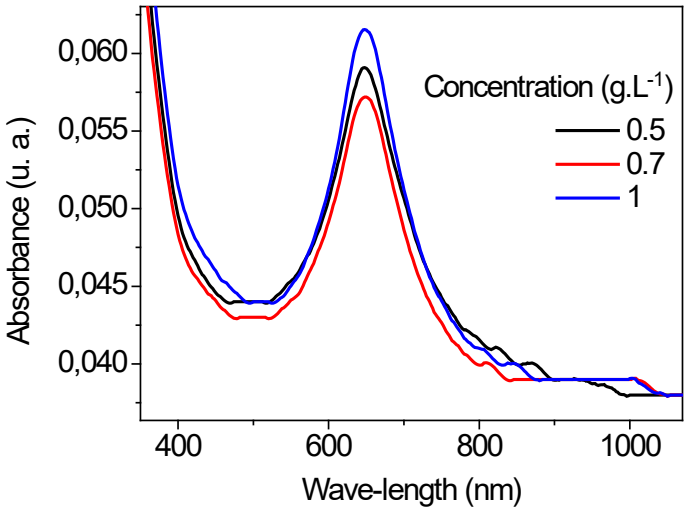

Figure 3. UV-Vis spectra obtained for PAH / FeTSPc modified substrate at pH 10.5, substrate contact time with 10 min solution at concentrations 1.0, 0.7 and 0.5 $g.L^{-1}$.

It can be seen in figure 4 that the pH variation does not provide a linear variation in the absorbance obtained, for example by raising the pH from 2.8 to 5.6 the absorbance value decreases, however, when the pH is increased from 8.2 to 10.5 an absorbance increases, corroborating with the non-linearity of the generating mathematical function.

.

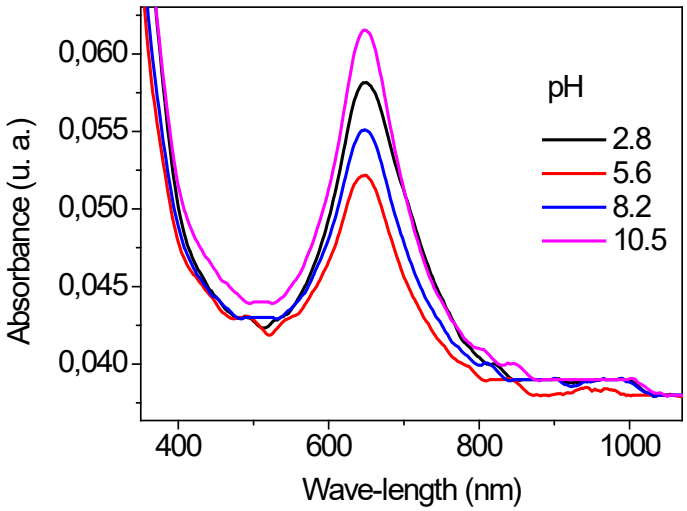

Figure 4. UV-Vis spectra obtained for PAH / FeTSPc modified substrate at 1 $g.L^{-1}$ concentration, substrate contact time with 10 min solution and pH 2.8 variation; 5.6; 8.2 and 10.5.

For the film obtained from FeTSPc solution at 1.0 $g.L^{-1}$ and pH 10.5, with only 10 minutes of contact with the substrate, the absorbance obtained was the maximum for this configuration (0.062 ua, Table 2), higher up to than those obtained when the contact time was increased, where, for example, at 90 minutes at pH 5.6, the absorbance obtained was only 0.047 water (Table 2). For the case where the FeTSPc solution at 0.5 $g.L^{-1}$ and pH 2.8, was used 10 minutes of contact with the substrate promoted the lowest absorbance (0.048 water) for this configuration, whereas when the contact, for example, for 90 minutes the absorbance was the maximum obtained (0.059 water) for this configuration. Linking these data without the use of computational or mathematical techniques can be very difficult, since, as discussed, by varying one of these parameters

(concentration, pH or contact time), the system has a different behavior. For this reason, this work sought to optimize the production of these films through intelligent tools, such as Artificial Neural Networks.

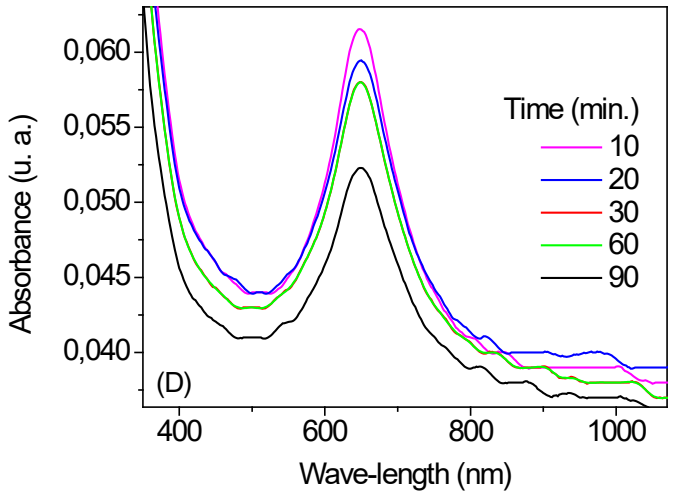

Figure 5. UV-Vis spectra obtained for the PAH / FeTSPc modified substrate at 1g.L^{-1} concentration at pH 10.5 and substrate contact times with the 10, 20, 30, 60 and 90 min solution**.**

3.2 Implementation of artificial neural network

With the implementation of an ANN, an intelligent system capable of performing interactions among all the input parameters was calculated, calculating the output corresponding to the desired response (absorbance), thus enabling the learning capacity of the network.

The definition of the stopping criterion is fundamental to the training of the network. Limit number of training cycles (number of epochs) or definition of a value for minimum error are used in some works [29].

When the training is stopped prematurely, the network may suffer the loss of generalization capacity, and when the training stop takes too long (too much training), it can memorize the examples presented, and thus lose its generalization capacity. Therefore, one of the most frequently used criteria for stopping network training is cross-validation.

Many training sessions were carried out with different configurations, where the number of training times equal to 200 was constant, the number of tests equal to 10 and cross-validations equal to 15, and only the learning rates were modified (Table 3). After the analysis of the resulting graphs, the algorithm verified the best configuration of the network to solve the problem addressed and the best learning rate, which is responsible for the best generalization response of the network, to provide satisfactory answers during the test for values not used during the training process. The networks were trained with different amounts of neurons in the hidden layer (s), wherein the first layer the number of neurons ranged from 2 to 7 and in the second, from 0 to 3 neurons.

Table 3. Configurations tested during ANN training.

Training	Configuration				Number of Neurons		Accuracy		
	Learning Rate	Training (%)	Validation (%)	Testing (%)	1ª Hidden Layer	2ª Hidden Layer	Training (%)	Validation (%)	Testing (%)
1	0.01	50	25	25	4	1	67	61	20
2	0.01	60	20	20	5	1	74	85	34
3	0.01	70	15	15	7	2	69	70	39
4	0.01	80	10	10	5	0	48	79	49
5	0.05	60	20	20	7	3	84	59	79
6	0.05	70	15	15	7	2	69	70	39
7	0.05	80	10	10	5	1	48	79	49
8	0.5	60	20	20	2	1	63	82	53
9	0.5	80	10	10	5	1	64	52	12

10	0.001	60	20	20	6	3	27	49	53
11	0.008	60	20	20	5	1	83	74	60
12	0.09	60	20	20	5	2	71	76	42
13	0.9	60	20	20	7	1	60	21	35

In Figure 6 we can visualize the results obtained for the 60:20:20 configuration (60% of the data used for training, 20% for validations and 20% for tests) using 0.01 as learning rate.

During the learning process of the network, the synaptic weights of the neurons are modified, forming a linear adjustment equation. Figure 6 shows the correlation between the results obtained and the desired outputs for the lowest least squares error ANN found.

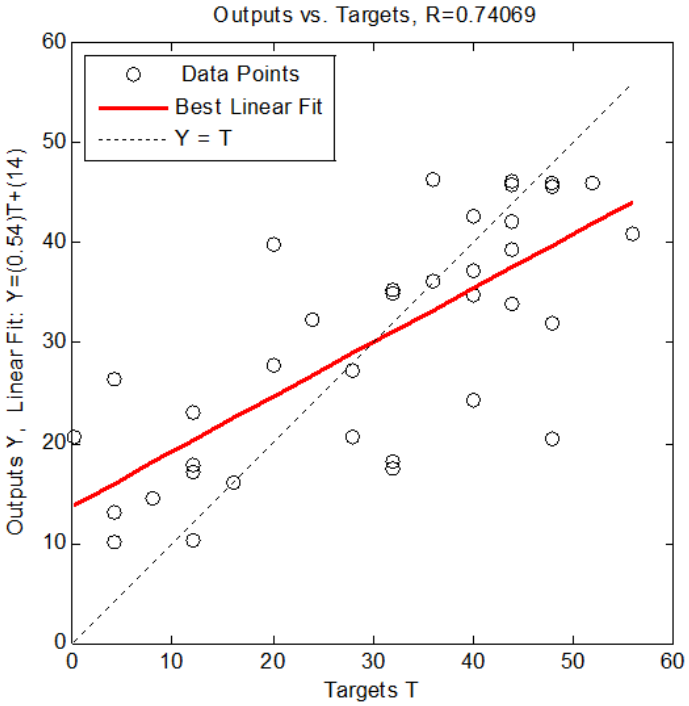

Figure 6. Comparison between the data obtained with those expected for each input set, forming the equation of the linear adjustment at each training stage for the ANNs for the 60:20:20 configuration with learning rate equal to 0.01, 5 neurons in the hidden first layer and 1 hidden second layer neuron.

As can be seen in Figure 6, the value obtained for R regarding percentage equals 74%. Analyzing the graph of Figure 7, we can see that it is essential to interrupt the training when the value of the cross-validation error remains stable for some periods after reaching its minimum value. This result probably means that during training the learning rate was meager. The learning rate influences the changes in the weights between the connections of the artificial neurons. Tiny learning rates (close to zero) imply long training time; however, high learning rates can cause oscillations around the solution, as seen in Figure VII.

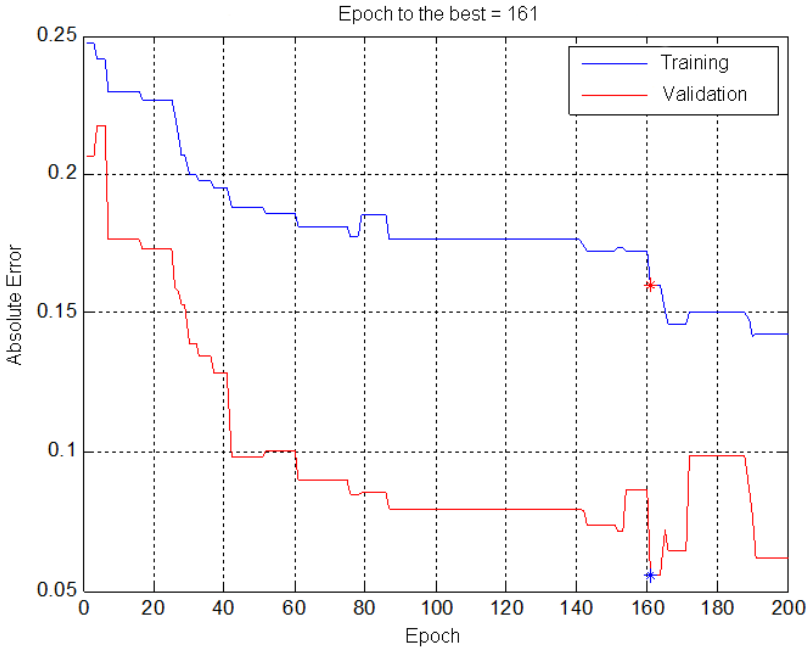

Figure 7. Absolute error graph for the training and validation set for the 60:20:20 configuration with learning rate equal to 0.01. The number of precise times until the smallest error is found (*).

With this in view, new training and execution of the algorithm were performed by changing the learning rate from 0.01 to 0.05, with the same configuration for the data set: 60% of the data for training, 20% for validation and 20% for the test. The following results are obtained (Figure 8 and Figure 9):

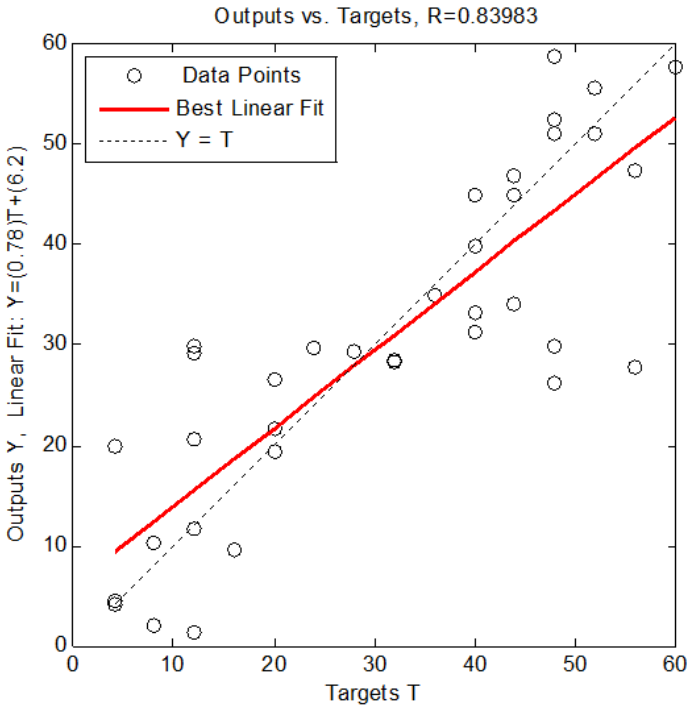

Figure 8. Comparison between the data obtained with those expected for each input set, forming the equation of the linear adjustment at each training stage for the ANNs for the 60:20:20 configuration with learning rate equal to 0.05, 7 neurons in the hidden first layer and 3 neurons in the second hidden layer.

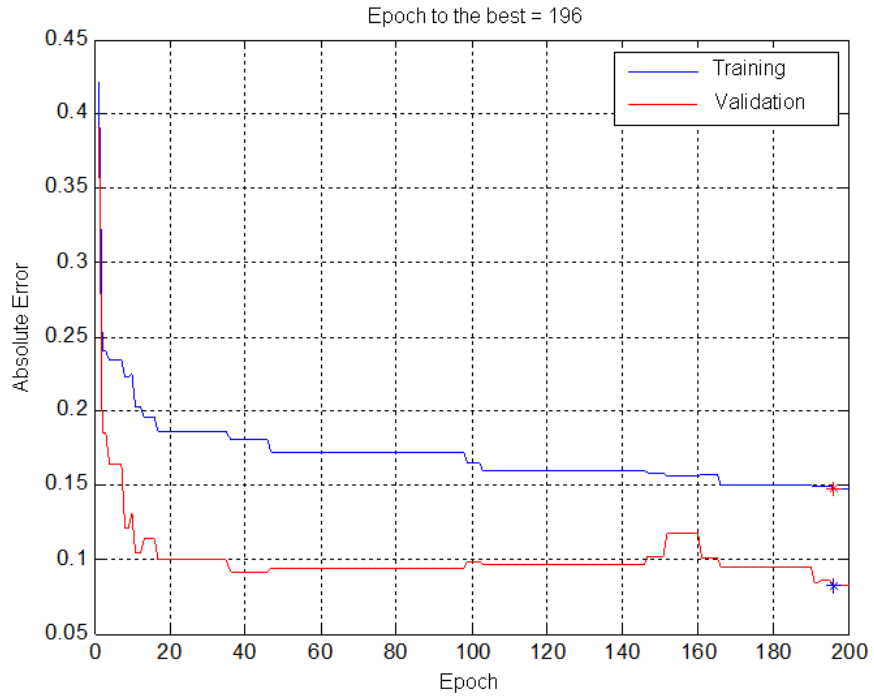

Figure 9. Absolute error graph for the training and validation set for the 60:20:20 configuration with learning rate equal to 0.05. The number of precise times until the smallest error is found (*).

Using the tests performed, ANN detected with the highest hit rate, and that is, the smallest mean square error has a 7:3:1 topology, i.e., seven neurons in the first hidden layer, three in the second hidden layer and one neuron in the layer (Figure 10).

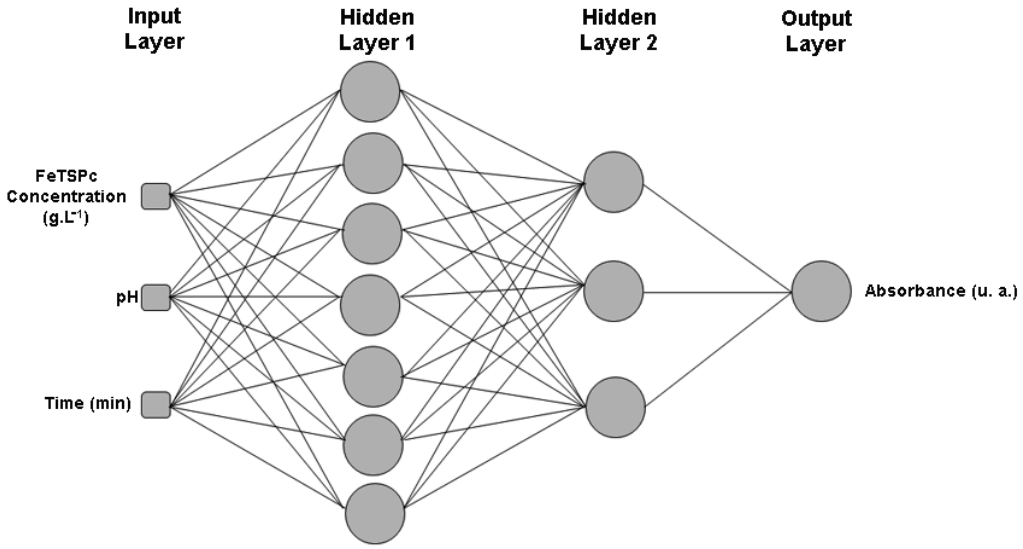

Figure 10. Schematic representation of the topology of the best ANN found by the cross-validation process.

The generalization capacity of ANN allowed the study of the importance of each parameter in the value of the absorbance obtained, increasing the studies and reducing the costs of time and material for the accomplishment of the experiments. With the application of the cross-validation technique, the best configuration for the neural network in this system was obtained (Figure 10), showing a correct degree of accuracy of 83.98%, measured by the correlation between the results calculated by ANN and experimental results.

The results obtained were evaluated using two different metrics: the correlation coefficient (R-value) and the percentage absolute mean error (MAPE). The first measure indicates how close the predicted results

are to the actual data. The second indicates the mean of all absolute percentage errors (Equation II), indicating the mean error size, expressed as a percentage of the observed value, regardless of whether the error is positive or negative. It is used to indicate the network hit rate.

$$MAPE = \frac{\sum_{k=1}^{n} \left| \frac{(Yd - Y)}{Yd} \right|}{n} \cdot 100 \qquad (II)$$

For the 60:20:20 configuration with a learning rate of 0.01, regarding MAPE, the results were 85.26, 74.06 and 34.21% for the validation, training and test sets, respectively (Figure 11).

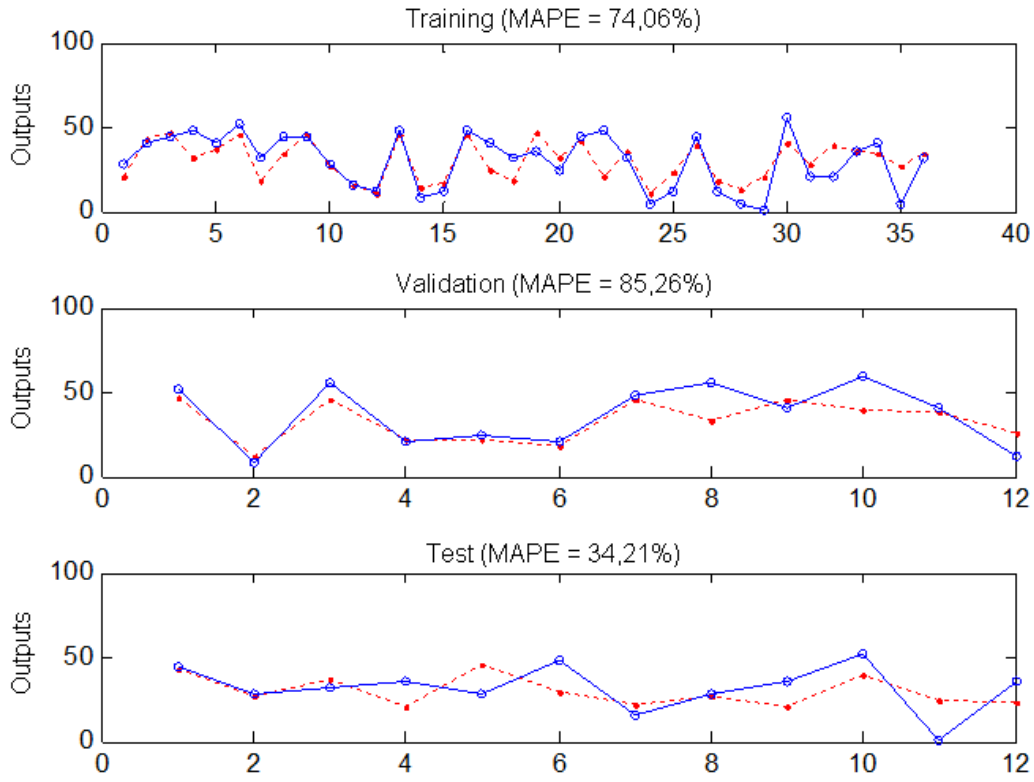

Figure 11. The result of data used in the training, validation and test sets for the 60:20:20 configuration with learning rate equal to 0.01. Desired Outputs (o) ANN Outputs (•).

For the 60:20:20 configuration with a learning rate of 0.05, regarding MAPE, the results were 58.82, 83.98 and 79.04% for the validation, training and test sets, respectively (Figure 12). Analyzing the graphs of Figure 12, we conclude the efficiency in the results provided by the best ANN found, both during the training phase and in the test phase, this means that the network was able to obtain a suitable generalization of the problem in predicting the absorbance value of a FeTSPc film from its experimental parameters.

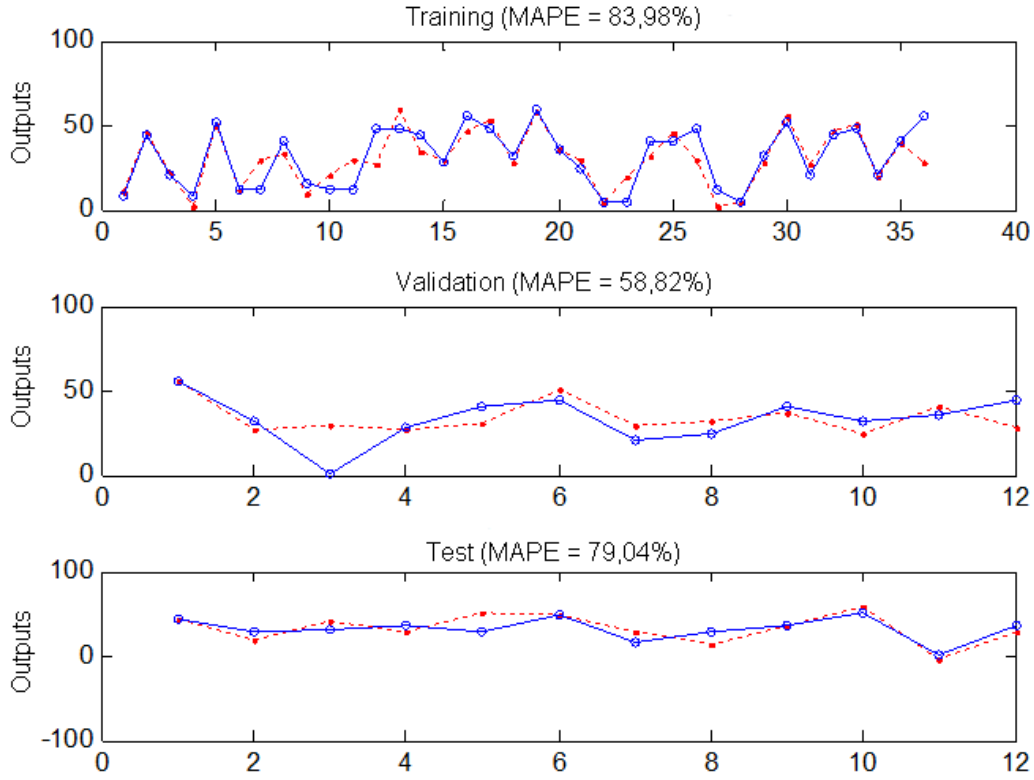

Figure 12. The result of the data used in the training, validation and test sets for the 60:20:20 configuration with a learning rate of 0.05. Desired Outputs (o) ANN Outputs (•).

During the process of validation and training of the network are calculated the absolute errors, which make it possible to affirm the best ANN and how many times it must be ready to be used. We obtained the best ANN topology using a mathematical comparison, which should be used to calculate the absorbance values obtained during the FeTSPc thin film production process (Figure 10).

4. Conclusions

The Artificial Neural Networks produced in this work were used in the construction of a predictive and optimized model for the calculation of the absorbance value obtained during the adsorption of FeTSPc in thin films self-layered by the Layer-by-Layer technique. The generalization of the ANN data enabled the development of a tool capable of calculating the values of the experimental parameters involved in the process of preparation of thin films to obtain films that present a higher value of absorbance based on the experimental parameters used.

The use of ANNs allows researchers in the area of materials and devices to create systems that simulate and reproduce thin film deposition processes.

Abbreviations

1.	ε	Molecular absorption or extinction coefficient
2.	A (I0 / I)	Absorbance
3.	a.u.	Arbritary unity
4.	ANTs	Artificial neural networks
5.	BK7	Glass slide
6.	BP	Backpropagation
7.	c	Concentration of absorbing material
8.	Epo	Number of epochs
9.	FeTSPc	Fe (II) tetrasulfonated Phthalocyanine
10.	$g.L^{-1}$	Gramas por Litro
11.	HCl	Hydrochloric acid
12.	KOH	Potassium hydroxide.
13.	l	Thickness of the sample through which light propagates
14.	LbL	*Layer-by-Layer*
15.	LMS	Least Mean Square
16.	MAPE	Mean Absolute Percentage Error
17.	Mili-Q	System used to obtain ultrapure water
18.	min	Minutes
19.	ml	Milliliter
20.	MLP	Multi Layer Perceptron
21.	mm	Milimiters
22.	$mol.L^{-1}$	Mol per Liter (unit of matter per liter)
23.	MSE	mean square error
24.	N_2	Nitrogen gas
25.	NaOH	Sodium hydroxide
26.	Neur	Number of neurons in the middle layer
27.	nm	Nanometer
28.	°C	Celsius Degree
29.	PAH	*Poly (allylamine hydrochloride)*
30.	Pc	Phthalocyanine
31.	pH	Hydrogen potential
32.	Rep	Number of repetitions (initialization)
33.	RMSE	Square root of the mean square error
34.	UV-Vis	Ultraviolet–visible spectroscopy

References

1. Tasso, T. T.; Furuyama, T.; Kobayashi, N. Absorption and Electrochemical Properties of Cobalt and Iron Phthalocyanines and Their Quaternized Derivatives: Aggregation Equilibrium and Oxygen Reduction Electrocatalysis. *Inorganic Chemistry*, 2013. v. 52, p. 9206-9215,

2. Adams, F. C.; Barbante C. Nanoscience, nanotechnology and spectrometry. *Spectrochimica Acta Part B: Atomic Spectroscopy*, **2013**. v. 86, p. 3-13,

3. Islam, N.; Miyazaki, K. Nanotechnology innovation system: Understanding hidden dynamics of nanoscience fusion trajectories. *Technological Forecasting and Social Change*, **2009.** v. 76, p. 128-140,

4. Idowu, M.; Chenab, J.-Y.; Nyokong, T. Photoinduced energy transfer between water-soluble CdTe quantum dots and aluminum tetrasulfonated phthalocyanine. *New J. Chem*., **2008.** v. 32, p. 290-296,.

5. Holder, E.; Langeveld, B. M. W.; Schubert, U. S. New trends in the use of transition metal-ligand complexes for applications in electroluminescent devices. *Advanced Materials*, **2005**. v. 17, p. 1109-1121,

6. Paton, A. S.; Morse, G. E.; Castelino, D.; Bender, T. P. Pseudohalides Sof boron subphthalocyanine. J. *Org. Chem*, 2012. v. 77, p. 2531-2536,

7. Centurion, L. M. P. C.; Moreira, W. C.; Zucolotto, V. Tailoring Molecular Architectures with Cobalt Tetrasulfonated Phthalocyanine: Immobilization in Layer-by-Layer Films and Sensing Applications. *Journal of Nanoscience and Nanotechnology*, **2012.** v. 12, p. 2399-2405,.

8. Crespilho, F. N.; Zucolotto, V.; Oliveira Jr, O. N.; Nart, F. C. Electrochemistry of Layer–by–Layer Films. Int. J. Electrochem. Sci, v. 1, p. 194-214, 2006.

9. Brinker, C. J.; Scherer, G. W. *Sol-gel Science the Physical and Chemistry of Processing. Academic Press, Boston*, 1990.

10. Nassar, E. J.; Ciuffi, K. J.; Gonçalves, R. R.; Messaddeq, Y.; Ribeiro, S. J. L. Filmes de titânio-silício preparados por "spin" e "dip-coating". *Química Nova*. 2003. v. 26, n. 5, p. 674-677,

11. Carvalho, C. L.; Varela, J. A. Construção e Caracterização de um Equipamento para Deposição de Filmes pela Técnica de Dip-Coating". *Revista de Física Aplicada e Instrumentação*, **2001**.v.14, n. 4, p.115-119,

12. Decher, G. Fuzzy nano-assemblies: toward layered polymeric multicomposites. *Science*, 1997. v. 277, p. 1232-1237,

13. Paterno, L. G.; Mattoso, L. H. C.; De Oliveira Jr, O. N. Filmes poliméricos ultrafinos produzidos pela técnica de automontagem: preparação, propriedades e aplicações. *Quím. Nova*, **2001**. v. 24, n. 2, p. 238–235,
14. Duran, N.; Matosso, L. H. C.; Morais, P. C. *Nanotecnologia: introdução, preparação e caracterização de nanomateriais e exemplos de aplicação*. Artliber, p. 13-68, 2006.
15. Rodrigues, M. C.; Muehlmann, L. A.; Longo, J. P. F.; Silva, R. C.; Graebner, I. B.; Degterev, I. A.; Lucci, C. M.; Azevedo, R. B.; Garcia, M. P. Photodynamic Therapy Based on Arrabidaea chica (Crajiru) Extract Nanoemulsion: In vitro Activity against Monolayers and Spheroids of Human Mammary Adenocarcinoma MCF-7 Cells. *Journal of Nanomedicine & Nanotechnology*, **2015**. v. 06, p. 1-6,.
16. Pereira, A. C.; Santos, A. S.; Kubota, L. T. Tendências em modificação de eletrodos amperométricos para aplicações eletroanalíticas. *Quím. Nova*, 2002. v. 125, n. 6, p. 1012-1021,.
17. Boni, L.; Piovesan, E.; Gaffo, L.; Mendonça, C. R. Resonant Nonlinear Absorption in Zn-Phthalocyanines. *The Journal of Physical Chemistry*. A, **2008** v. 112, p. 6803-6807,.
18. Vivas, M. G.; De Boni, L.; Gaffo, L.; Mendonca, C. R. Investigation of ground and excited state photophysical properties of gadolinium phthalocyanine. *Dyes and Pigments*, **2014.** v. 101, p. 338-343,.
19. Silva, L. G.; Neto, A. M. J. C.; Gaffo, L.; Borges, R. S.; Ramalho, T. C.; Machado, N. Molecular Dynamics of Film Formation of Metal Tetrasulfonated Phthalocyanine and Poly Amidoamine Dendrimers. *Journal of Nanomaterials*, **2013**. v. 2013, p. 1-7,.
20. Rocha, F. R. P.; Teixeira, L. S. G. Estratégias Para Aumento De Sensibilidade Em Espectrofotometria Uv-Vis. *Quim. Nova*, v. 27, n. 5, p. 807-812, 2004.
21. Santos, M. C.; Munford, M. L.; Bianchi, R. F. Influence of NiCr/Au electrodes and multilayer thickness on the electrical properties of PANI/PVS ultrathin film grown by LBL deposition. *Mater. Sci. Eng. B*, v. 177, n. 4, p. 359-366, **2012**.
22. Farias, E. A. O.; Dionisio, N. A.; Quemeles, P. V.; Leal, S. H. B. S. ; Matos de, J. M.; Silva Filho, E. C.; Bechtold, I. H.; Leite, J. R. S. A.; Eiras, C. Development and characterization of multilayer films of polyaniline, titanium dioxide and CTAB for potential antimicrobial applications. *Materials Science & Engineering*. **2014**. C, v. 35, p. 449-454,
23. Skoog, D. A.; West, D. M.; Holler, J. F.; Crouch, S. R. *Fundamentos de Química Analítica*, tradução da 8ª edição norte-americana, Editora Thomson, 2006.
24. Módolo, M. L.; Pessoa, A. C. Estudos eletroquimicos da Ftalocianina de Fe (II) imobilizada sobre a superficie da 3-n-Propilimidazol silica gel. In: XVII simpósio brasileiro de eletroquimica e eletroanalitica, 2009, Fortaleza. XVII simpósio brasileiro de eletroquimica e eletroanalitica, 2009.
25. Zucolotto, V.; Ferreira, M.; Cordeiro, M. R.; Constantino, C. J. L.; Moreira, W. C.; Oliveira JR., O. N. Electroactive layer-by-layer films of iron tetrasulfonated phthalocyanine. *Synthetic Metals*, **2003**. v. 137, p. 945-946,.
26. Silva, I. N., Spatti, D. H. E Flauzino, R. A. **Redes Neurais Artificiais: para engenharia e ciências aplicadas**. São Paulo: Artliber, 2010.
27. Engelbrecht, A. P. *Computational Intelligence: An Introduction*. 2nd Edition. Chichester: John Wiley, 2007. P. 628.
28. Lima, J. P. H.; Andrade, A. M.; Dirani, E. A. T.; Fonseca, F. J.; Bianchi, R F . Optimization of deposition parameters of POMA by spin coating using artificial neural networks. In: 3rd Brazilian MRS Meeting - SBPMAT, 2004, Foz do Iguaçu. Proceedings of 3rd Brazilian MRS Meeting, 2004.
29. Lima, J. P. H.; Andrade, A. M.; Dirani, E. A. T.; Fonseca, F. J.; Bianchi, R. F. Simulation and analysis of conductive polymers characteristics obtained by spin coating technique using artificial neural networks. In: 12th Brazilian Workshop on Semiconductor Physics, 2005, São José dos Campos. 12th Brazilian Workshop on Semiconductor Physics, 2005.
30. Noel, M. M.; Pandian, B. J. Control of a nonlinear liquid level system using a new artificial neural network based reinforcement learning approach. *Applied Soft Computing*, **2014**. v. 23, p. 444-451,.
31. Ferrari, K. R. S. A constrained integration (CINT) approach to solving partial differential equations using artificial neural networks. *Neurocomputing*, v.155, p. 277-285, 2015.
32. Zarpelon, F.; Galiotto, D.; Lovatel, R. H., Carli, L. N; Crespo, J. S.;Giovanela, M. Filmes finos de PAH/PAA decorados com nanopartículas de prata como potencial agente bactericida no tratamento microbiológico de efluentes industriais. XX Simpósio Brasileiro de Recursos Hídricos. Bento Gonçalves, 2013.
33. Kolmogorov, A. N. On the representation of continuous functions of several variables by superposition of continuous functions of one variable and addition. *Doklady Akademii Nauk*, v. 114, p. 679-681, 1957.
34. Oliveira, K. T.; Souza, J. M.; Gobo, N. R. S.; Assis, F. F.; Brocksom, T. J. Basic Concepts, and Applications of Porphyrins, Chlorins, and Phthalocyanines as Photosensitizers in Photonic Therapies. *Revista Virtual de Química*, **2015**. v. 7, p. 310-335,
35. Ferreira, A. P. M.; Dos Santos Pereira, L. N.; Da Silva, I. S.; Tanaka, S. M. C. N.; Tanaka, A. A.; ANGNES, L. Determination of α-Lipoic acid on a Pyrolytic Graphite Electrode Modified with Cobalt Phthalocyanine. *Electroanalysis* (New York, N.Y.), 2014. v. 26, p. 2138-2144,